



# Novel Self-expanding Shape-Memory Bioresorbable Peripheral Stent Displays Efficient Delivery, Accelerated Resorption, and Low Luminal Loss in a Porcine Model

Leonid Glushchenko, MD, Ph.D.<sup>1</sup> , Brad Hubbard, DVM<sup>2</sup>, Nikita Sedush, Ph.D.<sup>1</sup>, Vladislav Shchepochkin, Ph.D.<sup>1</sup>, Artur Krupnin<sup>1</sup> , and Aidar Sharafeev, MD, Ph.D.<sup>1</sup>

## Abstract

**Objective and Design:** The search for improved stenting technologies to treat peripheral artery disease is trending toward biodegradable self-expanding shape-memory stents that, as of now, still suffer from the acute trade-off between deliverability and luminal stability: Higher deliverability leads to lower lumen stability, vessel recoil, and stent breakage. This study was aimed at the development and testing of a self-expanding bioresorbable poly(L,L-lactide-co-ε-caprolactone) stent that was designed to produce confident self-expansion after efficient crimping, as well as quick bioresorption, and sufficient radial force.

**Materials and Methods:** Bench tests were employed to measure shape-memory properties, radial force, and hydrolytic degradation of the stent. The porcine model was employed to study deliverability, lumen stability, biocompatibility, and stent integrity. A total of 32 stents were implanted in the iliac arteries of 16 pigs with 15 to 180 day follow-up periods. The stented vessels were studied by angiography and histological evaluation.

**Results:** Recovery of the diameter of the stent due to shape-memory effect was equal to 90.6% after 6Fr crimping and storage in refrigeration for 1 week. Radial force measured after storage was equal to 0.7 N/mm. Technical success of implantation in pigs (after the delivery implemented by pusher) was 94%. At 180 days, no implanted stents were found to be fragmented: All of the devices remained at the site of implantation with no stent migration and all stents retained their luminal support. Only moderate inflammation and neointimalization were detected by histological assessment at 60, 90, 120, and 180 days. Lumen loss at 180 days was less than 25% of the vessel diameter.

**Conclusions:** The stent with the mechanical and chemical properties described in this study may present the optimal solution of the trade-off between deliverability and luminal stability that is necessary for designing the next generation stent for endovascular therapy of peripheral arterial disease.

## Keywords

self-expanding stent, bioresorption, shape memory, peripheral scaffold

## Introduction

Development of better stenting technologies for endovascular treatment of peripheral artery disease (PAD) is becoming increasingly prominent due to both clinical and technological factors.<sup>1</sup> Search for the concept of an ideal stent brought researchers to the acute trade-off between mechanical and clinical properties of the device.<sup>2,3</sup> As of today, drug eluting stents employed to treat PAD display 1 year restenosis rates of 23% to 42.9% after percutaneous transluminal angioplasty and 13.7% to 35% with additional stenting.<sup>1</sup> These rates constitute an impressive progress of PAD endovascular surgery, but must be further decreased.

One important consideration of the efficacy of bioresorbable scaffolds (BRS) is its deliverability.<sup>3</sup> Most stents today are delivered by balloon expansion that appears to add strain, injury, and inflammation to the vessel walls, and this play the major role in activating the restenosis. To

<sup>1</sup>Resotech Medical Solutions Corp, Delaware, USA

<sup>2</sup>Pathway Preclinical Services, Minneapolis, MN, USA

### Corresponding Author:

Leonid Glushchenko, Resotech Medical Solutions Corp, 51 Little Falls Drive, the City of Wilmington, County of New Castle, Delaware, 19808, USA.

Email: ileo.glu@gmail.com

**Table 1.** Diameter of Iliac Artery Vessels in the Studied Pigs.

Iliac artery diameter, mm	5.0–5.4	5.5–5.9	6.0–6.4	6.5–7.0
Number of vessels implanted	3	7	3	3

decrease these harmful effects, self-expanding stents with shape memory were developed. These stents are delivered to the vessel in the crimped state and later expand under the combination of body temperature and hydration.<sup>4,5</sup> Early experiments with self-expanding stents demonstrated improved functionality and efficiency, and hence today the ideal BRS appears to be a self-expanding shape-memory stent with high radial force and quick resorption.

The poly(L,L-lactide-co-ε-caprolactone) stent<sup>6–11</sup> was designed for this study to present 3 beneficial properties: (1) high deliverability based on high shape-memory expansion after the intensive crimping, (2) quick bioresorption, and (3) decreased tissue inflammation. All 3 benefits are provided by controlled molecular and supramolecular structure of the polymer material and production of the thin strut stent as described in the relevant patent application.<sup>12</sup> Preclinical studies of such stent pave an important avenue in the development of the BRS for the endovascular treatment of the PAD.

## Materials and Methods

The self-expanding peripheral stent was made of a semi-crystalline poly(L,L-lactide-co-ε-caprolactone) copolymer by laser cutting according to the technology described in the patent that illustrates production of the device.<sup>12</sup> The thermally-treated scaffold with a length of 21 mm and outer diameter (OD) of 8.5 mm has a closed cell structure, strut width of 200 μm (as in nitinol analogues) and thickness of 250 μm.

Radial force testing of the stent was performed with the use of RX650 Radial Force Tester (MSI, Flagstaff, AZ, USA). For better evaluation of radial and shape-memory properties, the testing was performed in 4 steps: (1) crimping to an OD of 2 mm at 42°C, (2) nitrogen cooling and 1 week storage in a refrigerator, (3) shape recovery in water at 37°C, and (4) evaluation of radial force by crimping of the recovered scaffold to an OD of 2 mm at 37°C.

Steps 1 and 2 simulate crimping of the scaffold onto a delivery system and storage before the implantation at low temperature, respectively. Steps 3 and 4 simulate scaffold expansion (due to shape-memory effect) in a vessel and a contact interaction between the scaffold and the vessel wall. At steps 1 and 4, the crimper was heated up to crimping temperature within 10 minutes. Radial force was evaluated as normalized (per unit length) force during the second crimping procedure (step 4) that caused 3% of irreversible (ie, plastic) deformation. Shape-memory properties were evaluated as a ratio of the scaffold OD after shape recovery 37°C to initial stent OD.

To perform hydrolytic degradation testing of the material in vitro, plates with a size 60 mm × 10 mm × 1 mm were fabricated by injection molding in HAAKE MiniJet Injection Molding System (Thermo Scientific, Waltham, MA, USA). During the degradation process at 37°C, we measured the decrease in the molecular weight and mass of the sample. The samples were immersed in 50 mL tubes with phosphate buffer of 7.4 pH with 0.2% NaN<sub>3</sub> (antibacterial agent). The average molecular weight ( $M_w$ ) was determined by size-exclusion chromatography on the Smartline gel permeation chromatography system equipped with refractometric detector (KNAUER, Berlin, Germany). Distilled tetrahydrofuran was used as an eluent. The experiments were performed at 40°C and 1 mL/min flow rate. The column was calibrated by polystyrene standards.

The stents were tested in 16 healthy model animals (pigs) without atherosclerotic lesions. Each pig was implanted with 2 stents (1 stent in the right common iliac artery and 1 in the left common iliac artery). In total, 32 devices were implanted using a 9Fr sheath introducer and pusher. The 9Fr sheath introducer was used because of the size of the scaffold, which is not suitable for 6Fr sheath. In future, the scaffolds will be crimped on a special 6Fr delivery device, which is currently under development. The stent diameter was 1–2 mm greater than the reference diameter of the vessel in the implantation zone. The diameter of iliac artery vessels in the studied pigs is shown in Table 1.

The animals were quarantined until the day of the study. The weight of the animals ranged from 60 to 70 kg; the age of the animals was commensurate to the weight. The pig model is recommended for the use in preclinical research in the FDA's (US Food and Drug Administration) "Guidelines for Presenting Research and Marketing Applications for Interventional Cardiology," May 1995. The testing center used the "Guide for the Care and Use of Laboratory Animals" (Institute of Laboratory Animal Resources, National Academy Press, 1996) as a guideline for animal care. All animals were fed standard high-fiber feed. There were no known impurities in the feed or water that could affect the results of this study. Animal care was performed in accordance with the protocol which was approved by the facility Institutional Animal Care and Use Committee.

Fasting was done 12 hours before surgery, water was allowed. After intramuscular injection of Zoletil for basic anesthesia, the tracheal intubation was performed, the skin was prepared, and the ear vein was established. After tracheal intubation, respiratory anesthesia was used.

During the operation, the animal was supine, with limbs fixed on the operating table, the surgical area on the thigh

**Table 2.** Stratification of the Trial Animals Based on the Research Time.

Control point	Days of trial	Number of pigs/stents (n)
1	15	16/32
2	30	16/32
3	60	16/32
4	90	12/24
5	120	8/16
6	180	4/8

shaved and disinfected, and the electrocardiogram (ECG) monitoring established.

The bilateral femoral arteries were surgically dissected and an 9Fr sheath was placed. Under the fluoroscopy, a 9Fr delivery sheath entered the femoral artery from the outer sheath tube and then entered the iliac artery along the guidewire. The size of the abdominal aorta and the bilateral external iliac artery was measured by angiography.

The degradable stent was placed at the end of the delivery sheath with the aid of the pushing rod. After positioned, the pushing rod was gripped, the delivery sheath was withdrawn, and the stent was released. Then the delivery sheath and the pushing rod were withdrawn. The position of the stent was further determined by angiography. The catheter sheath was withdrawn, and the femoral artery was ligated.

Aspirin (100 mg) and Plavix (75 mg) were administered daily after surgery, and antibiotics were given daily within 5 days after surgery. In total, 32 devices were implanted.

Each group of 4 experimental animals was followed up for 15, 30, 60, 90, 120, and 180 days. Calculation of stenosis in the stent was performed by diagnostic subtraction angiography (Table 2). During angiography, the reference diameter of the vessel, its structure and diameter, as well as the signs of thrombosis and restenosis of the stent were evaluated. At each control point of 60, 90, 120, and 180 days, a group of 4 pigs were sacrificed and histological evaluation of the vessel in the stenting area was performed. The molecular weight of the explanted devices was determined to evaluate the rate of biodegradation *in vivo*. The specimens were sectioned perpendicular to the axis of the vessel. Histological analysis was performed following hematoxylin and eosin staining, and observations were made under an optical microscope.

## Results

### Bench and In Vitro Degradation Tests

The recovery of the stent after crimping was evaluated by immersion in water at 37°C. Within 5 minutes after

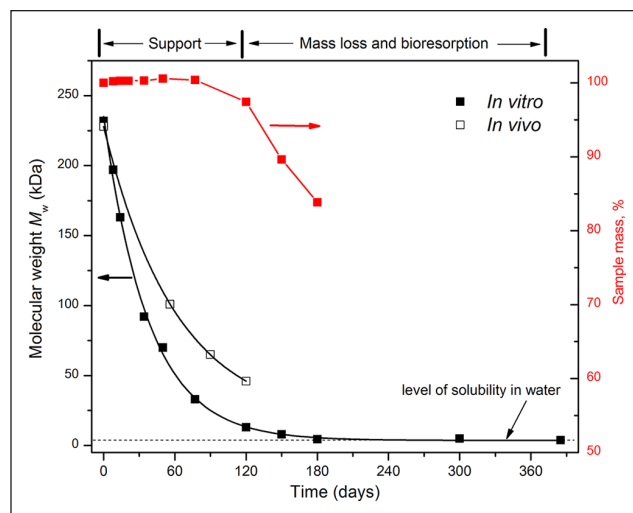


**Figure 1.** Hydrolytic degradation of the studied stent is demonstrated by the change of sample's mass (red squares), weight-average molecular weight of poly(lactide-co- $\epsilon$ -caprolactone) during hydrolytic degradation *in vitro* at 37°C (black squares), and biodegradation *in vivo* (empty squares). The hydrolysis of this material (a decrease in molecular weight) was rather fast and has started right from the first week of the experiment.

immersion, the stent recovers to an OD of 7.7 mm, which corresponds to 90.6% of the initial OD. The measured radial force of the stent after shape recovery and following crimping at 37°C was found to be 0.7 N/mm.

Hydrolytic degradation of poly(L,L-lactide-co- $\epsilon$ -caprolactone) used for creation of the stent revealed that the hydrolysis of this material (a decrease in molecular weight) was rather fast and began within the first week of the experiment (Figure 1). The weight-average molecular weight ( $M_w$ ) of the polymer decreased from 240 to 92 kDa in a month. However, this decrease in molecular weight is not crucial for mechanical properties of the material, which were retained at the same level. The mass of the sample increased slightly during the first weeks due to water absorption and remained approximately at the same level for 3 months. After 4 months of hydrolysis, the molecular weight decreased significantly and reached a critical value of 13 kDa. At this point, mechanical properties of the material have decreased, and water-soluble fractions of oligomers have started to wash out. This led to a reduction in the mass of the test sample to 97.5% of the original after 4 months of hydrolysis. A material of such a low-molecular weight is capable of disintegration even with a small effort. After 6 months, the sample mass was reduced to about 83% of the initial level. It was impossible to measure further mass loss due to mechanical rupture of the sample. The biodegradation kinetics of polymeric stents *in vivo* showed a similar pattern with a slightly lower rate. This may be due to a different environment and

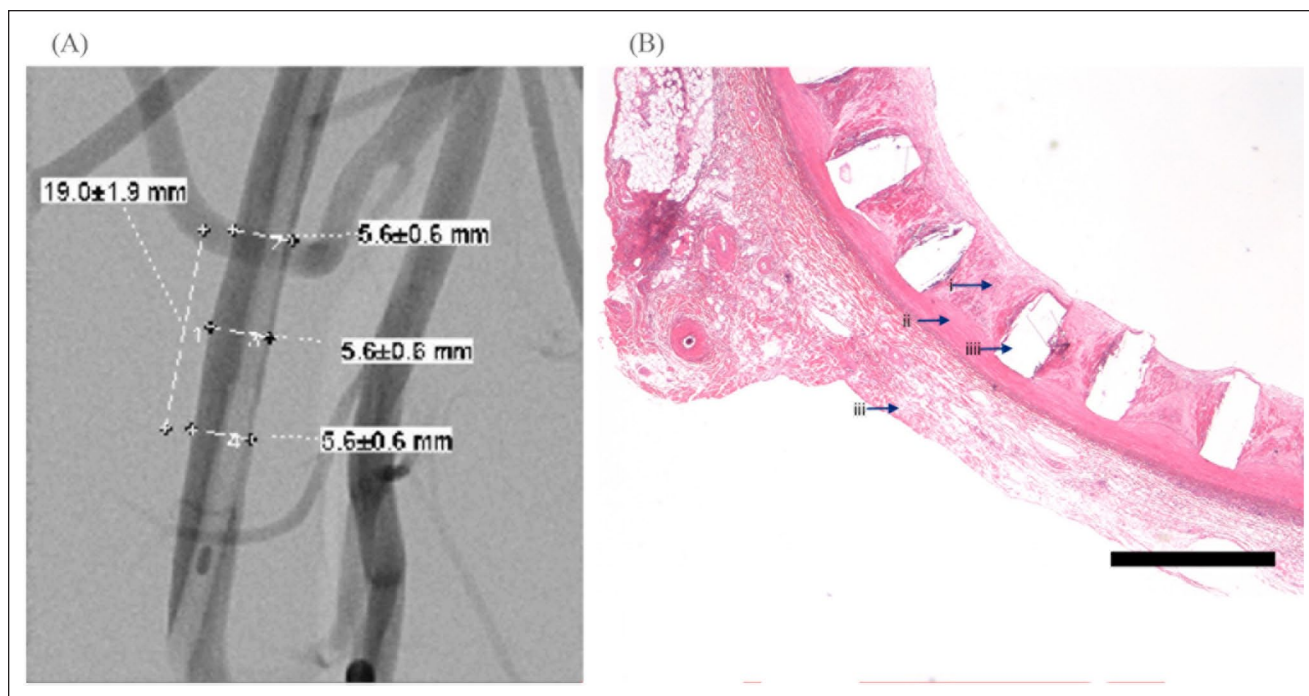


**Figure 2.** (A) Angiography 60 days post implant and histopathology of the left iliac artery. Angiography revealed irregularities in the contours of the artery. (B) Bar: 450  $\mu\text{m}$ . Arrows: (i) neointima, (ii) media, (iii) adventitia, and (iiii) strut holes. In the area of stent implantation, endothelialization of the stent is complete with a neointimal thickness of  $270 \pm 20 \mu\text{m}$ .

higher thickness of the model plates for in vitro test compared with stents. It is known that greater thickness of the device limits the rate of diffusion of low-molecular weight degradation products and leads to an auto-catalytic acceleration effect of hydrolysis.<sup>1</sup>

### In Vivo Results

The implantation success rate (performed with pusher) was 87.5% (deployment of the stent on the lines with the vessel's reference diameter). One case (6.25%) showed insufficient deployment of the stent, which required post-dilation. In another case (6.25%), the stent was damaged by the pusher. Implementation of a special device for delivery of the stent in the future should increase technical success of implantation up to 100%. All stents had satisfactory radiopacity and were well visualized against the background of iodinated contrast agents, even in the absence of radiopaque markers. An oversize of arteries was  $15\% \pm 2\%$  after implantation of stents.

Control angiography on the 15th and 30th days of the trial was performed in all 16 animals. In all cases, there was an increase in the diameter of the artery in the stent area by  $1.6 \pm 0.1 \text{ mm}$ , that means the effect of the stent "pre-expansion" within 30 days was recorded. Angiography of 1 animal (3%) showed lumen loss of the common iliac artery and stenosis which can be caused by neointimal proliferation. Despite the

small artery diameter and stenosis noted on the 15th day of investigation, on the 30th day of investigation the decrease of lumen loss and reopening of the vessel were observed. We conclude that the stent maintains its mechanical properties and radial stability.

Angiography of the 12 remaining animals on the 60th day follow-up period demonstrated further narrowing of the artery in 1 animal (6.25%). After angiography evaluation, 4 animals (8 stents) were taken out of the study (Figure 2A). According to the results of histological examination, there was less than 25% vessel stenosis and minimal inflammation. The stents retained their mechanical properties. In the area of stent implantation, neointima proliferation with a thickness of  $270 \pm 20 \mu\text{m}$  was detected (Figure 2B).

On the 90th day after stent implantation, angiography was performed in the second group of animals. Following final angiography, the animals were sacrificed and histopathology studies were performed (Figure 3A). Angiography of the iliac arteries of this group of animals did not show any abnormalities. Histopathology showed a slight narrowing of the vessel (less than 25%) and mild inflammation. In the area of stenting, neointimal proliferation with a thickness of  $350 \pm 50 \mu\text{m}$  was detected (Figure 3B).

On the 120th day of follow-up (5th Check Point), angiography and histopathology were performed for the 4 remaining animals. Angiography in 1 animal (6.25%)

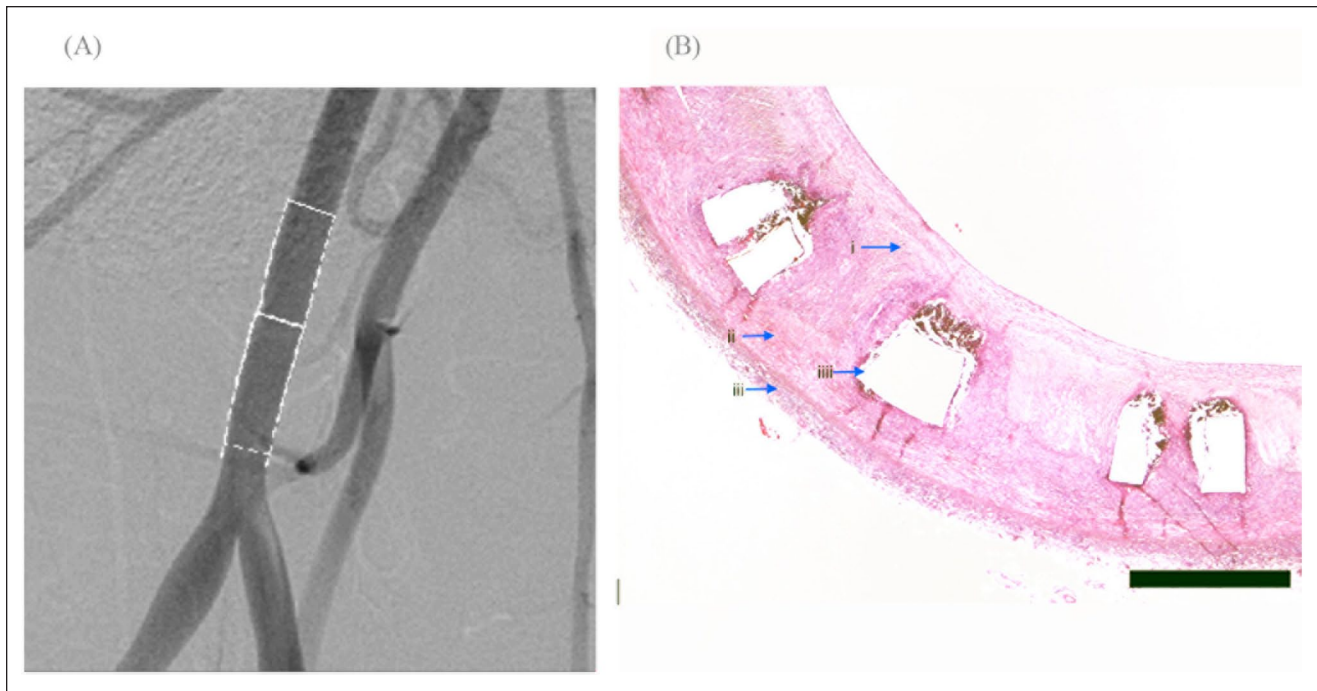


**Figure 3.** (A) Angiography and histopathology 90 days post implant in the right iliac artery. Angiography of the iliac arteries did not show any abnormalities. (B) Bar: 450  $\mu\text{m}$ . Arrows: (i) neointima, (ii) media, (iii) adventitia, and (iiii) strut holes. Histopathology showed a slight narrowing of the vessel (less than 25%) and a slight inflammation in the area of stenting. Complete endothelialization of the stent with a neointimal thickness of  $350 \pm 50 \mu\text{m}$  was detected.

showed a slight remodeling of the vessel with a decrease in the lumen of the vessel proximal to the implanted stent (in the area of the aortic bifurcation; Figure 4A). The molecular weight of the samples at this point was about 50 kDa. The stent was still mechanically stable at that time point. The results of hydrolytic degradation of the polymer material in vitro and biodegradation in vivo allow one to suppose that the stent completely degrades within 12–15 months after implantation. Histological evaluation of this area revealed a slight (less than 25%) decrease in the vessel lumen and signs of moderate inflammation. Histological evaluation of the vessel in the area of stenting revealed initial process of absorption without signs of inflammation and complete epithelialization of the stent with a neointima thickness of  $400 \pm 90 \mu\text{m}$  (Figure 4B).

Angiographically, visual abnormalities in the animals' arteries were not detected after 180 days (Figure 5A). Histological examination of this area did not reveal a decrease in the lumen of the vessel and signs of moderate inflammation. Histological evaluation of the vessel in the stenting area revealed partly endothelialization of the stent with a neointima thickness of  $520 \pm 100 \mu\text{m}$  (Figure 5B).

## Discussion

One of the key parameters of shape memory that we pursued in this study is the stable expansion of the stent after

deep crimping,<sup>11</sup> as inspired by the Tamai et al<sup>13</sup> stent, which was the first biodegradable stent implanted in human in 1999. We developed the bioresorbable stent based on poly(L,L-lactide-co- $\epsilon$ -caprolactone) copolymer that is described in the relevant patent applications.<sup>12</sup> Unlike poly(L-lactide), the developed copolymer has shape-memory property at body temperature ensuring self-expansion of a device after implantation.

Radial force of the stent was found to be 0.7 N/mm, which is enough for luminal stability as proven by in vivo tests in the porcine model. According to experimental and computational tests,<sup>14</sup> this value for designed stent is lower but comparable with the nitinol analogues (0.938 N/mm for Medtronic Complete SE (Medtronic, Ireland), 0.885 N/mm for Cordis SMART Control (Cordis, USA), and 0.936 N/mm for Boston Scientific Innova (Boston Scientific, USA)) and almost 2 times higher<sup>15</sup> than the radial force of poly(L-lactic acid) braided stent (0.4 N/mm).

Bench tests of the stent performed after crimping demonstrated 90% self-expansion due to shape-memory effect after immersion in water at 37°C for 3 minutes. This provides delivery of the device without balloon. Accelerated degradation of the material (compared with PLA) was another positive outcome of the modified molecular structure of the polymer. High mobility of polymeric chains in this state, as well as higher rate of hydrolysis, results in accelerated degradation. The in vitro tests showed that

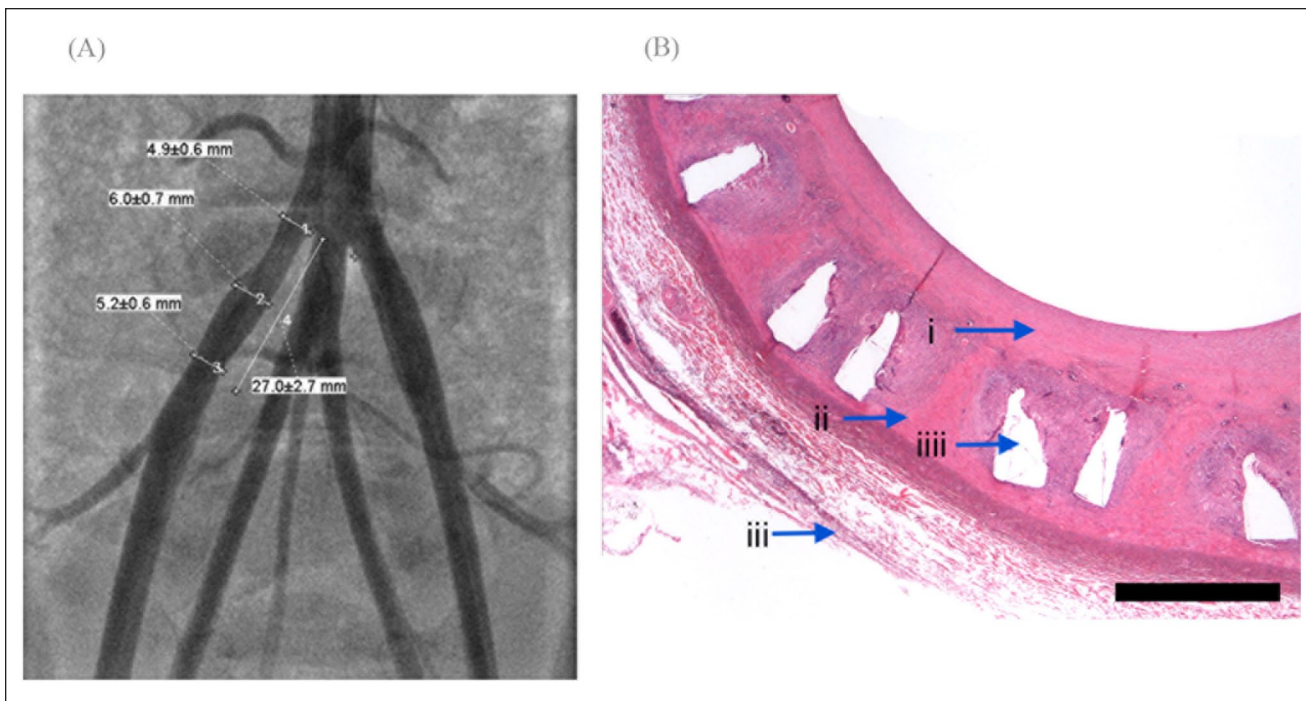


**Figure 4.** (A) Angiography and histological result 120 days after biodegradable stent implantation. The angiography showed a slight remodeling of the vessel with a decrease in the lumen of the vessel proximal to the implanted stent (in the area of aortic bifurcation). (B) Bar: 450  $\mu$ m. Arrows: (i) neointima, (ii) media, (iii) adventitia, and (iiii) strut holes. Histological evaluation of the vessel in the area of stenting revealed initial process of absorption without signs of inflammation. Endothelialization of the stent is complete with a neointimal thickness of  $400 \pm 90 \mu$ m.

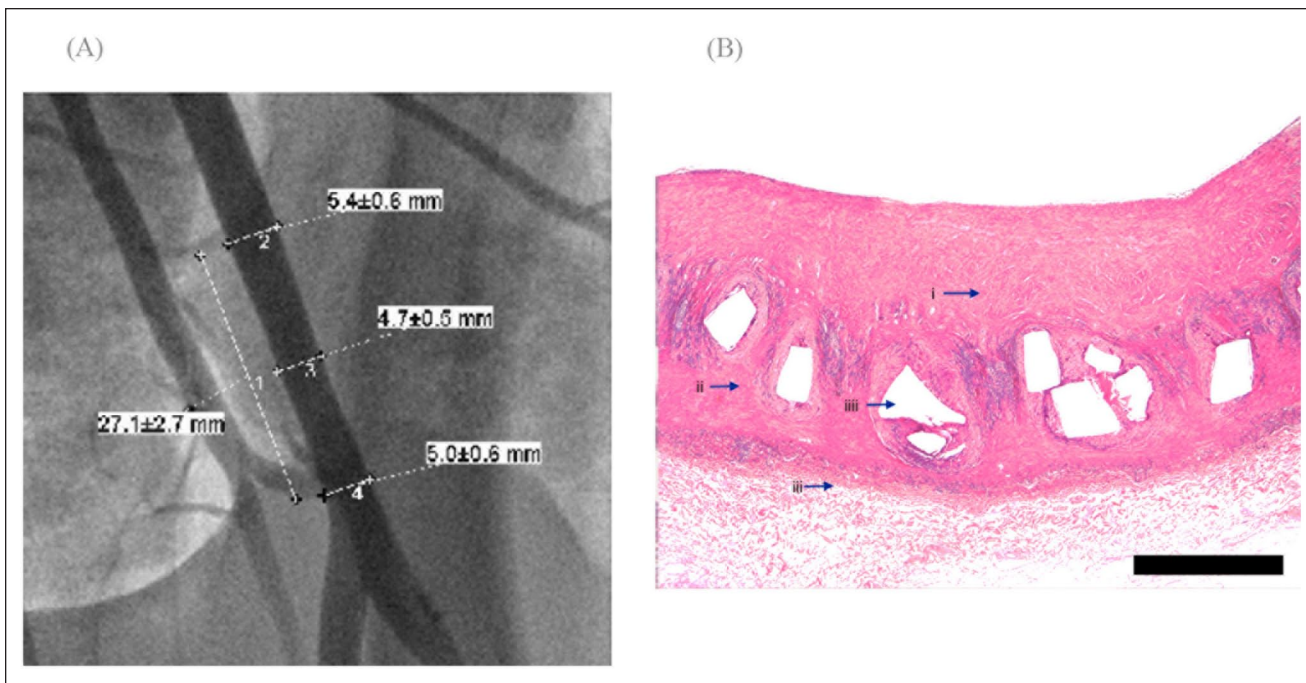


**Figure 5.** (A) Angiography and histological result 180 days after biodegradable stent implantation of the right iliac artery. No luminal loss is detected. (B) Bar: 450  $\mu$ m. Arrows: (i) neointima, (ii) media, (iii) adventitia, and (iiii) strut holes. Histological evaluation of the vessel in the stenting area revealed complete endothelialization of the stent with neointimal thickness of  $520 \pm 100 \mu$ m.

**Table 3.** Comparative Results on the Histographic Studies of Diverse Stents as Published in Zhao et al<sup>16</sup> with the Developed BRS With Shape Memory.

	3 months	6 months
Neointimal thickness, $\mu\text{m}$		
Bare Metal Stent (BMS) <sup>16</sup>	790 $\pm$ 200	730 $\pm$ 140
Drug Eluting Stent(DES) <sup>16</sup>	370 $\pm$ 400	410 $\pm$ 80
Bioresorbable scaffold(BRS) <sup>7</sup>	NA	NA
Bioresorbable scaffold BRS with shape memory	350 $\pm$ 50	520 $\pm$ 100
Endothelialization, %		
BMS <sup>16</sup>	100 $\pm$ 0.00	100 $\pm$ 0.00
DES <sup>16</sup>	100 $\pm$ 0.00	99.96 $\pm$ 0.04
BRS <sup>7</sup>	100 $\pm$ 0.00	100 $\pm$ 0.00
BRS with shape memory	100 $\pm$ 0.00	100 $\pm$ 0.00
Area stenosis, %		
BMS <sup>16</sup>	41.37 $\pm$ 6.73	38.80 $\pm$ 5.09
DES <sup>16</sup>	26.75 $\pm$ 1.29	27.25 $\pm$ 2.99
BRS <sup>7</sup>	9.1 $\pm$ 2.7	7.4 $\pm$ 5.6
BRS with shape memory	7.0 $\pm$ 2.4	6.5 $\pm$ 6.1

Abbreviations: BRS, bioresorbable scaffolds; NA, not available.

molecular weight of the polymer has decreased to a critical level after 4 months of hydrolysis. At this point, the drop in mechanical properties can be expected. However, the support for 3–4 months is enough for the remodeling of the vessel. The projected time for full bioresorption can be estimated as 13  $\pm$  3 months.

In vivo results demonstrate that the processes that followed implantation of the stent are quite typical. In all vessels, endothelialization has been fully completed by the 30th day. Only minimal initial resorption has been observed on the 90th day, while the start of the resorption has been manifested by the occasional cell infiltration in the stent rods, as observed histologically. The definitive resorption was observed at the 180th day, when only small fragments of the stent have been found intact. Neointima thickness was found to be 520  $\pm$  100  $\mu\text{m}$  at the 180th day. The resorption was accompanied by the moderate inflammation that signals acceptable biocompatibility of the stent during the entire duration of this resorption. Importantly, the stent has not migrated and stenosis has been insignificant (6.5%  $\pm$  6.1%), most probably related to the neointimal proliferation.

In vivo studies serve as an important demonstration of the stent safety that paves the way toward clinical trials. Although we did not employ comparables in our studies, the results may be quite accurately compared with the published results on the coated and non-coated nitinol stents,<sup>7</sup> as well as shape-memory BRS of Sharma et al.<sup>7</sup> Such comparison is summarized in Table 3. The inflammation levels that were induced by our stent are similar among all devices. The smaller stenosis area in our study, as compared with the other stents, may be explained by the larger arterial diameter of the animals used in our study. Most notably, our stent displayed a larger neointima thickness in comparison with

the Drug Eluting Stent (DES) device at the 180th day: 520  $\pm$  100  $\mu\text{m}$  versus 410  $\pm$  80  $\mu\text{m}$ . We believe that this difference does not jeopardize the advantages of our stent for 2 reasons: (1) we certainly will implement drug coating of our stent that will result in significant decrease of the neointima thickness during the initial period after implantation, and (2) these results cannot be compared directly, because our stent fully resorbs after 180th day while the DES stent continues to accumulate neointima thickness for many years ahead.

## Conclusion

The stent with the mechanical and biochemical properties described in this study may present the optimal solution of the trade-off between deliverability and luminal stability, which are necessary for designing the next generation stent for the endovascular therapy of PAD. Two key findings of this study are safety (low tissue inflammation) and low luminal loss of the proposed stent in the porcine model that, taken together, predict high patency in practical applications. Although this study did not include a control group, results still may be compared with those for nitinol stents<sup>16</sup> and the BRS of Sharma et al<sup>7</sup> to predict the relative superiority of the stent studied in this article in both safety and luminal loss. Another crucial advantage of the proposed stent is the significant improvement in deliverability due to self-expansion enabled by the polymer shape memory. Radial force of the stent is lower but comparable with nitinol analogues and almost 2 times higher than radial force of poly(L-lactic acid) self-expandable braided stent. Further clinical trials of such device on 6Fr delivery system are needed to investigate its actual patency.

## Acknowledgments

The authors would like to thank Professor Sergei Chvalun for many fruitful discussions.

## Declaration of Conflicting Interest


The author(s) declared the following potential conflicts of interest with respect to the research, authorship, and/or publication of this article: Leonid Glushchenko, Nikita Sedush, Artur Krupnin, and Vladislav Shchepochkin are authors of a patent and have royalties for its use. The patent protects intellectual property (IP) related to the stent, studied in this paper. Leonid Glushchenko, Vladislav Shchepochkin, Nikita Sedush, Artur Krupnin, and Aidar Sharafiev are shareholders of Resotech Medical Solutions Corp is a development company of researched devices. Brad Hubbard does not have any conflict of interest.

## Funding

The author(s) disclosed receipt of the following financial support for the research, authorship, and/or publication of this article: This work was funded by Resotech Medical Solutions Corp; Resotech Medical Solutions Corp paid for tests of devices, and Resotech Medical Solutions Corp was not involved in the decision to submit the manuscript for publication.

## ORCID iDs

Leonid Glushchenko  <https://orcid.org/0000-0001-7428-2264>

Artur Krupnin  <https://orcid.org/0000-0002-5674-4143>

## References

- van Haelst ST, Peeters Weem SM, Moll FL, et al. Current status and future perspectives of bioresorbable stents in peripheral arterial disease. *J Vasc Surg.* 2016;64(4):1151–1159.e1. doi:10.1016/j.jvs.2016.05.044.
- Watson T, Webster MWI, Ormiston JA, et al. Long and short of optimal stent design. *Open Heart.* 2017;4(2):e000680. doi:10.1136/openhrt-2017-000680.
- Ako J, Bonneau HN, Honda Y, et al. Design criteria for the ideal drug-eluting stent. *Am J Cardiol.* 2007;100(8B):3M–9M. doi:10.1016/j.amjcard.2007.08.016.
- Zhao F, Xue W, Wang F, et al. Composite self-expanding bioresorbable prototype stents with reinforced compression performance for congenital heart disease application: computational and experimental investigation. *J Mech Behav Biomed Mater.* 2018;84:126–134. doi:10.1016/j.jmbbm.2018.05.009.
- Ha D-H, Kim JY, Park TS, et al. Development of a radiopaque, long-term drug eluting bioresorbable stent for the femoral-iliac artery. *RSC Adv.* 2019;9(59):34636–34641. doi:10.1039/C9RA06179G.
- Toong DWY, Toh HW, Ng JCK, et al. Bioresorbable polymeric scaffold in cardiovascular applications. *Int J Mol Sci.* 2020;21(10):3444. doi:10.3390/ijms21103444.
- Sharma U, Concagh D, Core L, et al. The development of bioresorbable composite polymeric implants with high mechanical strength. *Nat Mater.* 2018;17(1):96–103. doi:10.1038/nmat5016.
- Wang R, Zhang F, Lin W, et al. Shape memory properties and enzymatic degradability of poly( $\epsilon$ -caprolactone)-based polyurethane urea containing phenylalanine-derived chain extender. *Macromol Biosci.* 2018;18(6):e1800054. doi:10.1002/mabi.201800054.
- Musiał-Kulik M, Gębarowska K, Kasperczyk J, et al. Bioresorbable copolymer of L-lactide and  $\epsilon$ -caprolactone for controlled paclitaxel delivery. *Acta Pol Pharm.* 2014;71(6):1023–1028.
- Yu X, Wang L, Huang M, et al. A shape memory stent of poly( $\epsilon$ -caprolactone-co-DL-lactide) copolymer for potential treatment of esophageal stenosis. *J Mater Sci Mater Med.* 2012;23(2):581–589. doi:10.1007/s10856-011-4475-4.
- Zhao F, Liu L, Yang Y, et al. The crimping and expanding performance of self-expanding polymeric bioresorbable stents: experimental and computational investigation. *Materials (Basel).* 2018;11(11):2184. doi:10.3390/ma11112184.
- US patent 11,096,808 B2 “Biodegradable Intravascular Shape Memory Stent”. August 24, 2021.
- Tamai H, Igaki K, Kyo E, et al. Initial and 6-month results of biodegradable poly-L-lactic acid coronary stents in humans. *Circulation.* 2000;102(4):399–404. doi:10.1161/01.cir.102.4.399.
- Brandt-Wunderlich C, Schmidt W, Grabow N, et al. Support function of self-expanding nitinol stents—are radial resistive force and crush resistance comparable? *Curr Dir Biomed Eng.* 2019;5(1):465–467. doi:10.1515/cdbme-2019-0117.
- Zhao G, Liu M, Deng D, et al. Effects of constraint between filaments on the radial compression properties of poly(L-lactic acid) self-expandable braided stents. *Polym Test.* 2021;93:1069640. doi:10.1016/j.polymertesting.2020.106963.
- Zhao HQ, Nikanorov A, Virmani R, et al. Inhibition of experimental neointimal hyperplasia and neoatherosclerosis by local, stent-mediated delivery of everolimus. *J Vasc Surg.* 2012;56(6):1680–1688. doi:10.1016/j.jvs.2012.04.022.